

Bubble acoustics: What can we learn from cetaceans about contrast enhancement?

T. G. Leighton, D. C. Finfer and P. R. White
Institute of Sound and Vibration Research
University of Southampton
Highfield, Southampton SO17 1BJ UK

Abstract—The profound effect of bubbles on the propagation of sound and ultrasound through liquids and tissue has meant that understanding of this process is key to a wealth of applications. These range from cases where that interaction is exploited (such as in the use of biomedical contrast agents) to circumstances where the potency of the effect massively hinders our capabilities (for example, the operation of sonar in coastal waters). The two diagnostic examples given above are revealing. The fact that in biomedicine the bubbles are exploited, whilst in the oceanic case they are problematic, stems from the readiness with which the biomedical field has embraced the concept of bubble nonlinearity, compared to the response of the sonar community, which relies upon linear propagation models. This is not because of differences in the abilities of the workers in the two fields, but rather for two more subtle reasons: first, the bubble size distribution for contrast agents is so well-known and well-constrained that researchers in the field need rely on little more than single-bubble models. This compares to the oceanic case, where the distribution of bubble radii will often span four orders of magnitude, will change dramatically over the course of a single measurement, and is often unknown. Indeed, the usual course in ocean acoustics is to appeal to historical datasets (often taken in vastly different environments, such as surf zone and deep water, with a wide range of windspeeds, fetch and air/sea temperatures etc.). These data provide some sort of estimate against which, for any given bubble size, it is hoped that the actual bubble number density does not vary by more than one order of magnitude. Second, the task in ocean acoustics would be to minimize the contribution of the bubbles to the detected signal and enhance the scatter from some other target. This undertaking is vastly more complicated than the task with biomedical ultrasonic contrast agents, which is to maximize the scatter from the bubble as opposed to the tissue. However there are intelligent creatures with a lifetime of experience of working in ocean acoustics, and generations in which to evolve techniques for coping with bubbly ocean water. This paper addresses the question of what physics would allow the cetaceans to do in bubbly ocean water in order to exploit the peculiar propagation conditions there. This question is particularly apt given that there are indeed instances where cetaceans generate bubbles in the water in order to facilitate their hunting. The question of whether cetaceans do indeed exploit the available physics is beyond the scope of this paper. However in discovering what techniques the physics would allow them to exploit, the opportunity opens up for humans to exploit the same techniques in order to enhance sonar in bubbly ocean water, and to enhance the exploitation of ultrasonic contrast agents.

Keywords-Bubbles, contrast agents, cetaceans, sonar, target

I. INTRODUCTION

Acoustics affects our lives profoundly and commonly, both as a nuisance and a necessity. Through speech, acoustics has dominated our communications for millennia. It underpins not only recorded music but also live transmissions, from entertainment in theatres and concert venues to public address systems. Although our experience has for generations been dominated by audiofrequency sound in air, today we use ultrasound in liquids for biomedical diagnosis and therapy, for sonochemistry and ultrasonic cleaning, and for the monitoring and preparation of foodstuffs, pharmaceuticals and other domestic products. From the Second World War to the present conflicts, acoustics has had an unrivalled role in the underwater battlespace. Underwater sound sources are used to map petrochemical reserves and archaeological sites, as well as to monitor a huge variety of important commercial and environmental features, from fish stocks to climate change. In all these examples, gas bubbles are the most potent naturally-occurring entities that influence the acoustic environment in liquids [1-3]. However our experience as humans of audiofrequency sound in air does not equip us with an intuitive appreciation of the acoustic environment in liquids. The mammals with greatest experience of this are cetaceans (whales, dolphins and porpoises). Given the complexity and potency of gas bubbles in liquids, and the potential for their exploitation, this paper addresses the question of whether there is anything we can learn from the acoustical response of cetaceans to the bubbly marine environment. Within the range of observed behaviours, most curious of all is the aptitude of cetaceans purposefully to generate vast clouds of bubbles via their blowholes. This is because, compared to man-made sonar, the sonar 'hardware' of cetaceans has been described as being mediocre [4]. Hence if they possess no more understanding than that used by humans in processing sonar signals in bubbly environments, in creating such bubble clouds cetaceans are effectively blinding their own sonar. However certain aspects of cetacean behaviour, particularly when they hunt, suggest that at times the bubbles they generate may be enhancing their acoustic capabilities. The acoustic and mental processing that might be involved is explored through the use of a new model for nonlinear acoustic propagation in bubbly water, in order to explore to what extent these possibilities may reflect upon our own exploitation of bubbles in marine and biomedical ultrasonics.

II. THE COASTAL ENVIRONMENT AS CETACEANS MIGHT SEE IT

Coastal ocean waters provide an acoustic environment which is far more complicated than that encountered with diagnostic biomedical ultrasound. Even the simplest models indicate surroundings which have great potential to confuse anyone relying on active acoustic sonar. In Fig. 1(a) only the two most simple (i.e. time-invariant) acoustic scatterers in the coastal water column are included: the sediment and the air/water interface (both modeled as plane static reflectors). Even here a single target turns into a multitude (with appropriate time/phase delays). The case when the observer is itself the source of sound is particularly fascinating. A sound source in a wedge-shaped coastal waters can ‘perceive’ image sources; were such a simple wedge ever to exist, one can, for example, imagine how a single cetacean might see this as a ring of ‘siblings’.

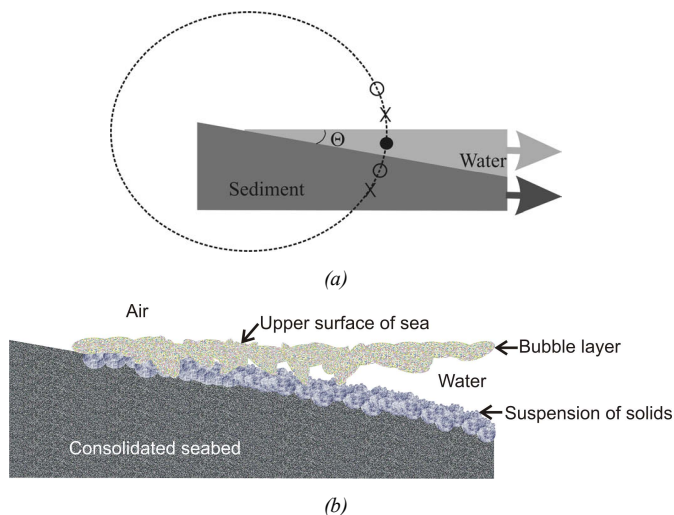


Figure 1. (a) If a coastal zone can be approximated by a wedge shape of ocean, with a bottom which reflects acoustic pressure waves with no phase change, and an air/water interface which reflects them with π phase change, then for frequencies high enough for a ray approach to be valid, the net sound field built up in the water by an object (●) emitting sound will be that which would be produced were the object in free-field, and sound were in addition emitted image sources either in phase (○) with the original source, or in antiphase (×).

The sediment and atmosphere boundaries of the water column being flat acoustic mirrors in this model, in the 2D plane passing vertically through the source these images will be distributed around the circle shown by the dashed line. The first few image sources are shown (○,×). For certain wedge angles Θ (such as the 15° used here) the sources map onto discrete sites on the dashed circle. (b) In this more realistic diagrammatic representation of the coastal zone, both the sea-air interface and consolidated seabed are more complicated reflectors than in (a). The air/sea interface will not only undulate with the passing of surface waves, but be punctuated with the noisy entrainment of bubble clouds. These bubbles can persist for many minutes against buoyancy, forming a dynamic sub-surface bubble layer which will attenuate and scatter acoustic signals (potentially nonlinearly), and can alter the sound speed by $\pm 50\%$ or more. Likewise, the near-bottom suspended solids will scatter and attenuate sound travelling near the sea-bed, and may contain trapped gas which has attached itself to the solid particulate grains.

Of course most coastal regions do not resemble the flat-sided wedge of Fig. 1(a). Real ocean coastlines provide features whose optical equivalents would be stranger than a carnival ‘hall of mirrors’ [2], its floor covered by a fluctuating ‘dry-ice fog’ (the optical equivalent of suspended sediment particles), its wedge-shape complicated by ripples on the

mirrored floor. Its ceiling would be an undulating, highly reflecting mirror, in some places focusing the sound in moving ‘hot spots’ within the water column and floor, and in other places producing areas of dark, absorbing bubble clouds covered with a bright speckle of resonant bubble scatterers. Imagine those clouds being explosively generated by a breaking wave, then spreading over time. The optical equivalent of monostatic or bistatic sonar might involve one or more people with flashlights in this otherwise dark ‘hall of mirrors’. The optical equivalent of nonlinearity would be if the flashlight emitted a strongly-attenuated red light in the carnival hall of mirrors; when, to compensate for this, the brightness of the flashlight is increased, blue new colours might be generated (the optical production of second-harmonic production, though of course the frequencies of blue light in the optical analogue is not twice that of red).

The development of human underwater sonar throughout the 20th Century concentrated on acoustic problems relevant to the deep-water threats which characterized the Cold War. However since the end of the Cold War, coastal waters have been of prime importance. Sonar expertise needs to develop to cope with this more challenging environment, which can for example hide mines that can be relatively inexpensive, threaten civilian shipping and personnel as well as military, and which can interfere with operations if their absence or locations cannot be confirmed (Fig. 2) [1]. With these new challenges has however come an impetus to explore how the transformation of acoustic propagation by complex environments may be used as a diagnostic tool for characterising that environment, from our oceans to off-world environments [1,3].

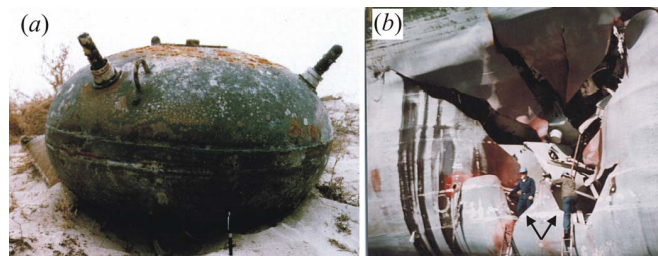


Figure 2. (a) An LUGM-145 (available for \$1900) carries a 660 kg charge and is based on a pre-First World War design. Such mines are usually moored on a chain, or drift on the surface, and are set off by contact with a ship. Modern mines are triggered by a ship’s magnetic, acoustic or pressure signature (or combination of the above) so that they cannot readily be cleared by dummy contact methods. (b) Around \$5 million of damage was caused to the *USS Tripoli* (LPH-10) after it struck an LUGM-145 moored contact mine during operation Desert Storm. Two personnel are arrowed for scale. (DSTL were consulted before reproduction of this image.)

Marine mammals often inhabit such coastal waters, and their acoustic emissions often propagate through bubbly water. Such bubbles can be generated under breaking waves or wakes, through biological decomposition, or even by the mammals themselves. Two circumstances are of particular interest: the possible use of acoustic signals to trap prey in bubble nets; and the ability of dolphin sonar to operate in bubbly water (such as the surf zone) that would confound the best man-made sonar [4].

III. THE BUBBLE NETS OF HUMPBACK WHALES

For many years there has been speculation as to the mechanism by which humpback whales (*Megaptera novaeangliae*) exploit bubble nets to catch fish [5]. It has been known for decades that single whales, or groups, dive deep and then swim in an upward spiral, releasing bubbles (Fig. 3(a)) to form the walls of a cylinder, the interior of which is relatively bubble-free (Fig. 3(b)). The prey are trapped within this cylinder, for reasons previously unknown, before the whales lunge feed on them from below (Fig. 3(c)). It is usually assumed that prey are contained by the bubbles alone. However it is certainly known that when humpback whales form such nets, a proportion (as yet unquantified) of them emit very loud, ‘trumpeting feeding calls’, the available recordings containing energy up to at least 4 kHz. Leighton *et al.* [5] proposed that these whales may be using such calls to enhance the ability of their bubble nets to trap the fish, in the following manner. A suitable void fraction profile would cause the wall to act as a waveguide. Assume the scales permit the use of ray representation. Fig. 4(a) shows how, with a hypothetical tangential insonification, the mammals could generate a ‘wall of sound’ around the net, and a quiet region within it (Fig. 4(b)). The natural schooling response of fish to startling by the intense sound as they approach the walls would, in the bubble net, be transformed from a survival response into one that aids the predator in feeding [1]. The frequencies in the feeding call are indeed in the correct range to excite resonances in fish swim bladders and, given their sensitivities, presumably such excitation could discomfort the fish sufficiently for it to return to the interior of the net.

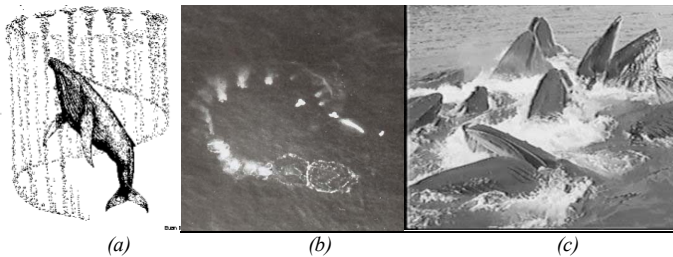


Figure 3. (a) Schematic of a humpback whale creating a bubble net. A whale dives beneath a shoal of prey and slowly begins to spiral upwards, blowing bubbles as it does so, creating a hollow-cored cylindrical bubble net. The prey tend to congregate in the centre of the cylinder, which is relatively free of bubbles. Then the whale dives beneath the shoal, and swims up through the bubble-net with its mouth open to consume the prey (‘lunge feeding’).

Groups of whales may do this co-operatively (Image courtesy of Cetacea.org). (b) Aerial view of a humpback bubble net (photograph by A. Brayton, reproduced from [6]). (c) Humpback whales lunge feeding (Image courtesy of L. Walker, <http://www.groovedwhale.com>)

Fig. 4(b) plots the raypaths from four whales whose beam patterns are represented by a 10° fan of 281 rays, for a bubble net in which the void fraction increases linearly from zero at the inner and outer walls, to 0.01% at the mid-line of the wall. The proposed ‘wall of sound’ and quiet interior are clearly visible. Even if the whales do not create sufficiently directional beams and insonify tangentially, the bubble net might still function through its acoustical effects. The ‘wall of sound’ effect in Fig. 4(b) is generated from those rays which impact the wall at low grazing angles. Those rays which never

impact the wall do not contribute to the ‘wall of sound’. If rays of higher grazing angle impact the net, they may cross into the net interior, though their amplitudes would be reduced by the bubble scattering, and attenuation alone would generate a quieter region in the centre of the net.

The actual acoustics of the cloud will of course be complicated by 3D effects and the possibility of collective oscillations, and of tuning calls to match the size of the net [5]; and even, speculatively, bubble-enhanced non-linear effects [5] which might be utilized by whales, for example to reduce beamwidth or generate harmonics, sum- and difference-frequencies *etc.* [1,5]. Suffice to say, the whales deliberately generate a bubbly environment and exploit it to hunt, and the physics would allow a wide range of possibilities for exploiting acoustics to enhance that hunt.

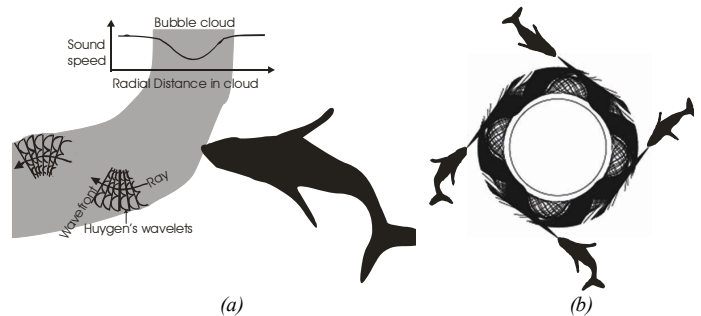


Figure 4. (a) Schematic of a whale insonifying a bubble-net (plan view; sound speed is least at the mid-line of the net wall). (b) Four whales insonify bubble net (the inner circle demarcates the inner boundary of the net wall; the outer boundary is obscured by rays). See Leighton *et al.* [2] for details.

IV. DOLPHIN USE OF BUBBLE NETS

The previous section discussed how some humpback whales may have found acoustic techniques for enhancing the performance of their bubble nets. They are not alone in using bubble nets to catch prey. Some dolphins have also been observed to feed using bubbles (Fig. 5) [1,7]. However *Odontoceti* regularly exploit frequencies in excess of 100 kHz for echolocation. At such frequencies the bubble nets influence the sound field in a very different manner to that shown in Fig. 4(b), most notably generating strong scattering and severe attenuation ($>200 \text{ dB m}^{-1}$ at 100 kHz, compared to only $\sim 6 \text{ dB m}^{-1}$ for the 4 kHz component used by humpback whales in bubble nets).

This creates a dilemma. In creating bubble nets, either the dolphins are blinding their sonar when they need it most (i.e. when hunting in a visually complex environment); or they have sonar systems which out-perform the best man-made sonar. Given that dolphin sonar hardware has unremarkable specifications compared to the best man-made sonar [4], if their sonar is operational in bubble nets, it must be a result of the platform characteristics, the processing, or both. Given the high amplitude pulses dolphins can generate ($>50 \text{ kPa}$ zero-to-peak at 1 metre range), and the short ranges over which they are required to detect prey in bubble nets, it is conceivable that they are exploiting a nonlinearity. At such short ranges, the ability of the dolphin rapidly to move its acoustic projector and sensors provides a system for insonifying a target through a

range of angles, and indeed dolphins have been observed to move their heads from side to side as they approach a target [8]. This, coupled with their ability to generate many pings in rapid succession, puts together a series of characteristics which would be of great value in a system which exploits nonlinearities in target detection. Such a proposition will now be explored.

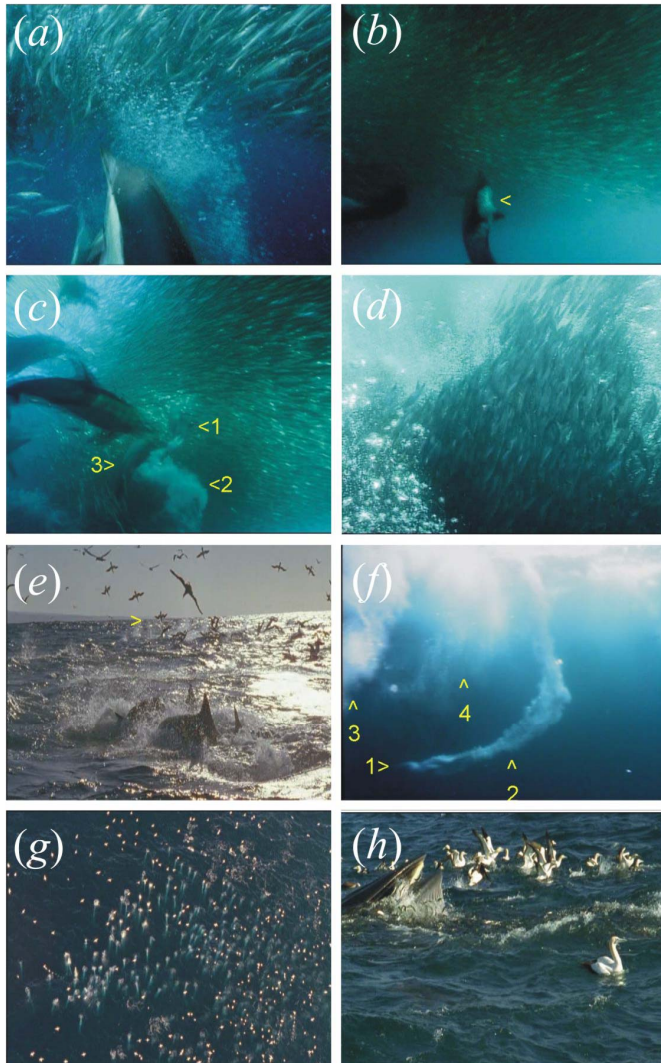


Figure 5. (a) Common dolphins herd sardines with bubble nets. (b) A dolphin starts to release a cloud of bubbles (arrowed) from its blowhole. A moment later (c) this dolphin (1) swims on, leaving behind the expanding cloud (2). Other dolphins (including the individual labeled '3') enter the frame. (d) The sardines school within a wall of bubbles that they are reluctant to cross, whilst (e) gannets dive into the sardine shoal to feed (arrowed). (f) On diving, a gannet (1) entrains a bubble plume (2). Plumes a few seconds old (3, with an older 4) have spread. (g) An aerial view shows hundreds of tight bubble plumes beneath airborne gannets. (h) A Bryde's Whale joins the feed. It surfaces with open mouth, which it then closes, sardines spilling from it. Images copyright of the The Blue Planet (BBC) and reproduced with permission. The accompanying book to the series is Byatt *et al.* [7].

Many dolphins and porpoises echolocate using frequencies on the order of 100 kHz [4], where attenuation in bubbly water can be on the order of 100 dB m⁻¹ [12]. However such estimates of attenuation assume that the bubbles undergo linear

pulsations in the steady state, whereas dolphins can exploit short pulses of sufficiently high amplitude to drive bubbles into nonlinear oscillation. Even without any special processing, attenuation can be dramatically reduced if nonlinear propagation occurs and, once nonlinearities have been generated, even very rudimentary processing can enhance the contrast between the nonlinear bubbles and a linearly-scattering target. For example, if the receiver is narrowband, then energy scattered by a bubble in harmonics at higher frequencies than the incident beam will, of course, be 'invisible' to such a detector. Furthermore, if the bubble population falls within a certain range of power law distributions, even a wideband receiver could detect sonar enhancements resulting from the reduced absorption which the bubble nonlinearity provides. Additionally, there may be further gains if more sophisticated processing is considered [9].

It is very possible that, for dolphin and porpoise sonar to operate effectively in bubbly water, the dolphins could mentally be undertaking signal processing which takes into account the nonlinearities they are generating [1,9]. This is because, as introduced earlier, although the best human sonar hardware is superior to that available to dolphins and porpoises [4], these cetaceans manage to echolocate in environments (bubbly water, sediments etc.) which confound the best man-made systems. The processing must therefore be making the difference. Given the severe scattering, attenuation and reverberation the dolphins and porpoises must be counteracting, a nonlinear process would seem to be a strong possibility. The following section introduces the method by which this possibility can be quantitatively explored.

V. MODELING THE NONLINEAR PROPAGATION OF SHORT ACOUSTIC PULSES IN BUBBLY WATER

In 1989, Commander and Prosperetti [10] summarised the most widely-used scheme for predicting the propagation characteristics of an acoustic wave through bubbly liquids. It assumes linear steady-state bubble pulsations in response to a monochromatic driving field. Leighton *et al.* [11,12] developed a theoretical framework into which any single-bubble model could be input, to provide propagation characteristics (*e.g.* attenuation and sound speed) for a polydisperse bubble cloud (which may be inhomogeneous) incorporating whatever features (*e.g.* bubble-bubble interactions) are included in the bubble dynamics model. Because of the inherent nonlinearity, such a model cannot make use of many familiar mathematical tools of linear acoustics, such as Green's functions, complex representation of waves, superposition, addition of solutions, Fourier transforms, small-amplitude expansions *etc.* The crux of this model is in the summation of the volume responses of the individual bubbles to the driving pressures. If the bubble cloud is divided into volume elements, let dP_l be the change in the pressure applied to the l th volume element as a result on an incident ultrasonic field. Divide the polydisperse bubble population into radius bins, such that every individual bubble in the j th bin is replaced by another bubble which oscillates

with radius $R_j(t)$ and volume $V_j(t)$ (about equilibrium values of R_{0j} and V_{0j}), such that the total numbers of bubbles N_j and total volume of gas $N_j V_j(t)$ in the bin remain unchanged by the replacement. If the bin width increment is sufficiently small, the time history of every bubble in that bin should closely resemble $V_j(t) = V(R_{0j}, t)$ (the sensitivity being greatest around resonance). Hence the total volume of gas in the l th volume element of bubbly water is:

$$V_{g_l}(t) = \sum_{j=1}^J N_j(R_{0j}, t) V_j(t) = V_{c_l} \sum_{j=1}^J n_j(R_{0j}, t) V_j(t), \quad (1)$$

where $n_j(R_{0j}, t)$ is the number of bubbles per unit volume of bubbly water within the j th bin. From this scheme Leighton *et al.* [12] identified a parameter, defined as:

$$\xi_{c_l} \approx c_w / \sqrt{1 - \rho_w c_w^2 \sum_{j=1}^J n_j(R_{0j}) (dV_j/dP_l)}. \quad (2)$$

Crucially this ξ_{c_l} provides a *generic framework into which any bubbly dynamics model may be inserted* (giving $dV_j(t)/dP_l(t)$ appropriate to bubbles in free field or reverberation [13], *in vivo* [14], in structures or sediments, or in clouds of interacting bubbles, *etc.* as the chosen model dictates).

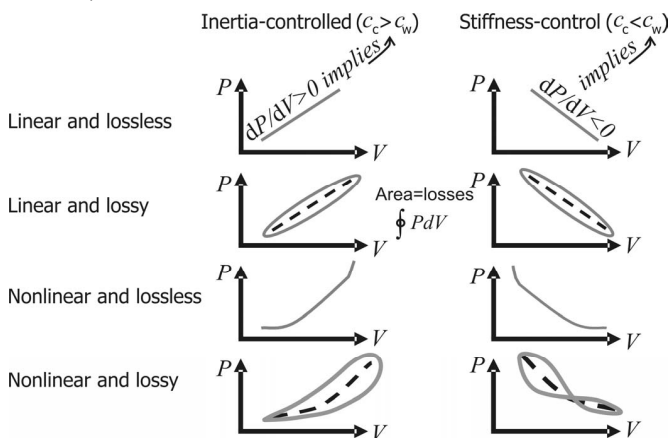


Figure 6. Schematics of steady-state bubble volume oscillations vs. applied pressure. The left column shows the result for the inertia-controlled regime, and the right column corresponds to the stiffness controlled regime. The four rows correspond to conditions which are (from top downwards): linear and lossless; linear and lossy; nonlinear and lossless; nonlinear and lossy.

To illustrate this, consider a monodisperse bubble population pulsating in the linear steady-state (Fig. 6). If the propagation were linear and lossless, the graphs of applied pressure (P) against bubble volume (V) would take the form of straight lines. The location of the bubble wall would be plotted by the translation of the point of interest up and down these lines at the driving frequency (Fig. 6, top row). Since a positive applied pressure compresses a bubble in the stiffness-controlled regime, here $dV/dP < 0$ (Fig. 6, top row, right). If, in this linear lossless regime, ξ_{c_l} (2) is seen as equivalent to c_c (the sound speed in the bubbly water), then $c_c < c_w$. However

since a π phase change occurs across the resonance, the opposite is true in the inertia-controlled regime (Fig. 6, top row, left). The sound speed in a polydisperse population can be found through addition of such gradients as directed by the formula for ξ_{c_l} (2). If conditions are linear and lossy (Fig. 6, second row), each acoustic cycle in the steady-state must map out a finite area which is equal to the energy loss per cycle from the First Law of Thermodynamics [12]. The characteristic spine (dashed line, Fig. 6, second row) of each loop can, through summation as directed by the formula for ξ_{c_l} , give the sound speed in a polydisperse population. This is effectively equivalent to the approach of Commander and Prosperetti [10], although they characterised the problem using a complex wavenumber, rather than through the locus in P - V space. If conditions are nonlinear and lossless, in steady-state the P - V graphs will depart from straight-lines (for example because the degree of compression cannot scale indefinitely; Fig. 6, third row). The gradient dV/dP varies throughout the acoustic cycle in a manner familiar from nonlinear acoustic propagation, and appropriate summation (as in ξ_{c_l}) can appropriately describe this propagation and the associated waveform distortion. If conditions are nonlinear and lossy, finite areas are mapped out, and whilst the characteristic spines may present significant challenges, nonlinear propagation may again be identified (the example of the right of the bottom row in Fig. 6 illustrates a strong second harmonic, where the steady-state volume pulsation undertakes two cycles for each period of the driving field).

The generation of such second harmonics is of course well-known when high amplitude acoustic fields are passed through bubbly liquid, and can readily be predicted by the new theoretical framework for the prediction of the acoustic propagation of arbitrary waveforms through bubbly media (Fig. 7). This has been applied to both oceanic bubbles [12] and to ultrasonic contrast agents [14]. In the use of contrast agents, the exploitation of nonlinearities to enhance the scatter from the bubbles, compared to that from tissue, is a far simpler problem than the enhancement of scattering from a target compared to that from bubbles, particularly where the bubble size distribution resembles those typical of ocean environments. These issues will be discussed in the following section.

VI. USE OF QUADRATIC NONLINEARITY TO ENHANCE TARGET DETECTION

One route for exploiting the nonlinearity to enhance target detection relies on the generation of even-powered terms in the expansion of the nonlinearity associated with the scatter from the bubble. Having identified a strong second harmonic, and noting that such even-powered harmonics would be insensitive to the sign of the driving field, Leighton [1,12] suggested that the use of closely-spaced pulses of opposite polarity could enhance the detection of prey with respect to bubbles. Fig. 8 illustrates just one of the ways in which the linear scatter from targets such as swim bladders driven off-resonance, or mines, might be enhanced compared to the scatter from oceanic bubble clouds. If the returned time series is split in half, then on subtraction of these two halves, the signal from the linearly scattering target doubles, whilst the energy invested in the

even-powered harmonics of the scatter from the bubbles is suppressed (Fig. 8). Of course the linear and odd nonlinear terms will not be suppressed. This means that, when this technique is used to enhance the detection of linearly scattering targets compared to detection of bubbles, it will not be as effective as the converse. That is to say, it is not as effective as the enhancement of bubble scatter, compared to that from linearly scattering targets, which occurs when the two halves of the time series are added. This is a general feature of many of the possible nonlinear enhancement techniques, and may be exploited for contrast agents.

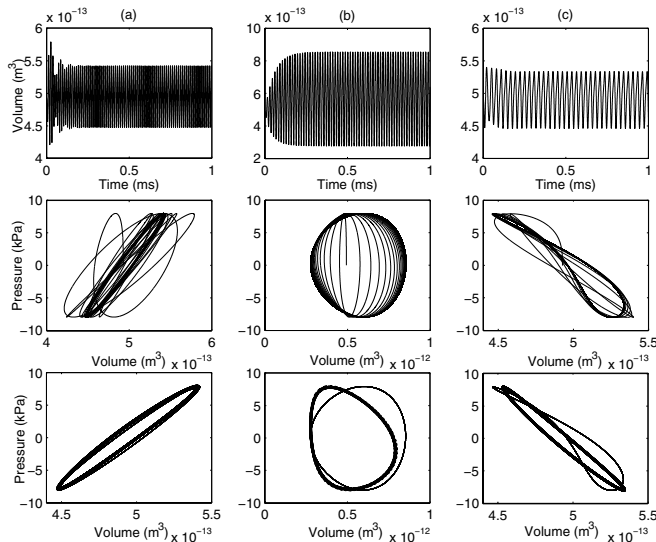


Figure 7. Bubble responses for a 49 μm bubble insonified by a semi-infinite pulse starting at $t=0$ with an amplitude of 7.95 kPa at (a) 84.2 kHz (b) 65.7 kHz and (c) 31.5 kHz. The top graph in each case shows the volume time history calculated using the Keller-Miksis equation (with appropriate representations for thermal, viscous and radiation losses) [12]. The middle graph in each case shows the corresponding pressure-volume curve. The darker area in each PV curve shows the steady state regime, where the successive loci overlap each other. Nonlinear components will cause crossovers in a loop (as in the middle and bottom rows of Fig. 7(c), where a second harmonic arises from driving the bubble close to half resonance frequency). The bottom row superimposes the steady-state loops of the middle row (thin line) with the corresponding linear solution using the steady-state formulation of Commander and Prosperetti [10] (thick line). From Leighton *et al.* [12].

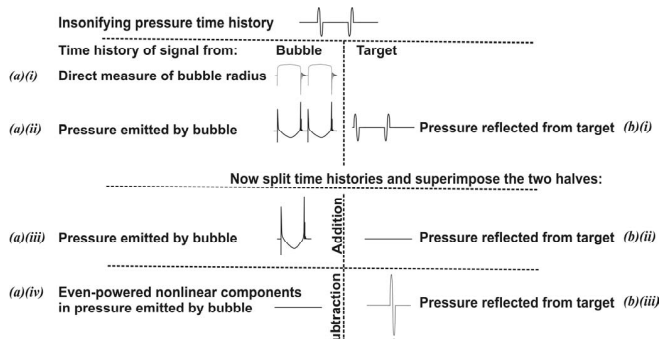


Figure 8. Schematic of a proposed 'Twin Inverted Pulse Sonar', whereby the scattering from a linear scatterer (such as a fish or a mine), and scattering from nonlinear scatterers (such as bubbles) can be enhanced and suppressed relative to one another.

Let us say the problem is to detect a linearly scattering object (the 'target') which is difficult to detect because it is immersed in a cloud of bubbly water. Such a target might be a fish in a dolphin bubble net - even with a swim bladder, the fish would produce ostensibly linear scatter from dolphin echolocation because the gas is driven at frequencies which are much greater than resonance. Alternatively, it might consist of a military mine which is a hazard to landing craft because it is hidden from sonar by breaking waves.

Consider if the emitted sonar signal were to consist of two high amplitude pulses, one having reverse polarity with respect to the other (Fig. 8, top line). Linear reflection from the solid body is shown in Fig. 8(b)(i). The bubble generates nonlinear radial excursions (Fig. 8(a)(i)) and emits a corresponding pressure field (Fig. 8(a)(ii)). Whilst the pressure emitted by the bubble may contain linear and odd-powered nonlinearities, it is the even powered (*e.g.* quadratic) nonlinearities which will be insensitive to the sign or the driving pulse, and hence which can be used to enhance the scatter from the target over that from the bubbles. It is these quadratic (and high even-powered components) which will be discussed in Fig. 8, and below.

Normal sonar would not be able to detect the signal from the solid (Fig. 8(b)(i)), as it is swamped by that from the bubbles (Fig. 8(a)(ii)). If however the returned time histories are split in the middle and combined to make a time history half as long, enhancement and suppression occurs. If the two halves of the returned signals are added, the even-powered nonlinear components of the scattering from the bubble are enhanced (Fig. 8(a)(iii)), whilst the signal from linearly scattering target is suppressed (Fig. 8(b)(ii)). This can be used to enhance the scatter from biomedical contrast agents. If however the two halves of each returned signal are subtracted from one another, the even-powered nonlinear components of the scattering from the bubbles is suppressed (Fig. 8(a)(iv)) whilst the reflections from the solid body are enhanced (with the usual constraints imposed by increased signal-to-noise ratio) (Fig. 8(b)(iii)).

If echolocation is the equivalent of vision underwater, then switching from linear to nonlinear sonar in bubble clouds might find analogy with driving through fog. 'Linear headlamps' would provide the familiar backscatter from the fog, making detection of targets difficult (analogous to the intense sonar backscatter from bubbles). However switching to nonlinear sonar might be equivalent to turning on 'nonlinear headlamps' in a car, which backscatter far less from the fog and so make driving easier. A preliminary calculation suggests that this technique may have potential to enhance the detection of linearly scattering targets in bubble clouds. Fig. 9 shows two driving pulses which are used to insonify a bubble: one has negative polarity with respect to the other.

Fig. 10 shows the linear scatter from the target (above the dashed line, in (a) and (b)), and the scatter from a bubble (below the dashed line, in (c) and (d)) [15]. The graph on the left in each case (*i.e.* (a) for the target; (c) for the bubble) shows the scatter from the pulses from Fig. 9: the upper plot (i) shows the scatter when excited by the 'positive' pulse of Fig. 9(a); the lower plot (ii) shows the scatter when excited by the 'negative' pulse of Fig. 9(b).

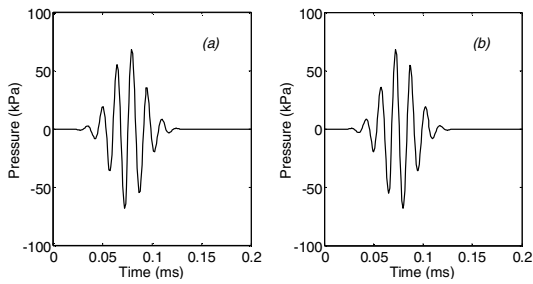


Figure 9. The two driving pulses (centre frequency 65.7 kHz) used to insonify a bubble: the (a) ‘positive’ pulse has negative polarity with respect to (b) the ‘negative’ pulse.

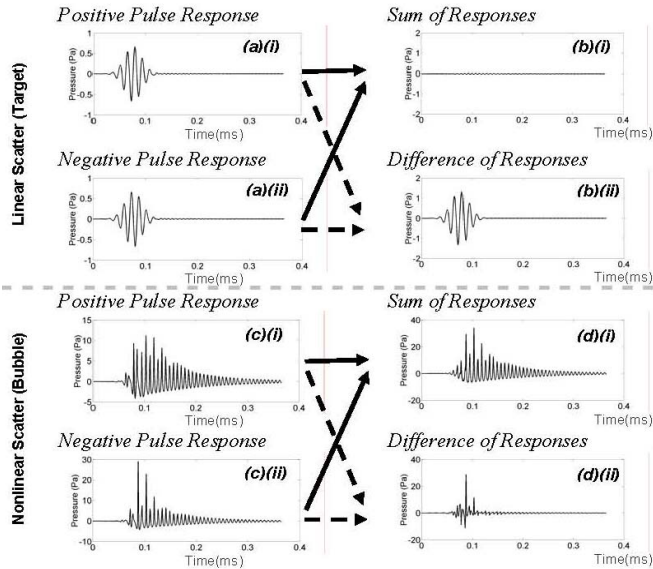


Figure 10. Scatter after insonification by pulses of Fig. 9, with linear scatter from the target (above the horizontal dashed line, in (a) and (b)), and the scatter from a single bubble (below the horizontal dashed line, in (c) and (d)). The air bubble has radius 22.5 microns and is in water under a static pressure of 1 bar. The centre frequency of the insonifying pulses (Fig. 9) is therefore at half the bubble pulsation resonance frequency. The graph on the left in each case ((a) target; (c) bubble) shows scatter from the pulses from Fig. 9: the upper plot (i) shows scatter when excited by the ‘positive’ pulse of Fig. 9(a); the lower plot (ii) shows the scatter when excited by the ‘negative’ pulse of Fig. 9(b). Solid arrows indicate addition, dashed arrows indicate subtraction.

The linear scatter of the positive pulse (Fig. 10(a)(i)) is in antiphase with that from the negative pulse (Fig. 10(a)(ii)), so that they add (the process indicated by the upper pair of solid arrows lines in Fig. 10) they produce zero signal (the time history in Fig. 10(b)(i) is not precisely zero because of numerical errors). When they are subtracted from each other (the process indicated by the upper pair of dashed arrows in Fig. 10), the amplitude of the signal is doubled, which is of course equivalent to a 6 dB increase over the energy in either of the original signals in (a). However the nonlinear scatter by the bubble of the positive pulse (Fig. 10(c)(i)) is not in antiphase with that from the negative pulse (Fig. 10(c)(ii)). Indeed, when they add (the process indicated by the lower pair of solid lines in Fig. 10) they produce a signal (the time history in Fig. 10(d)(i)) which is 5 dB greater than the average energy of the original signals in (c). When they are subtracted from

each other (the process indicated by the lower pair of dashed lines in Fig. 10), the amplitude of the signal is 1 dB less than the average energy of the original signals in (c) [15]. The key point to note here is that addition of signals in Fig. 10 enhances the scatter of the bubbles compared to the linear scatter from the target; whilst subtraction does the opposite, enhancing the signal from the linearly scattering target compared to that of the bubbles. That it is easier to enhance the detection of bubbles compared to the linearly scattering target, than to do the converse, is of course expected, given that the bubble signal does not consist of purely even-powered nonlinearities. There are very many ways in which the nonlinearity generated by the bubbles may be exploited to enhance sonar detection of a linearly scattering target. If the receiver is narrowband, that proportion of energy which is at harmonics that are outside of the receiver is sufficiently great to detect these harmonics, their higher frequencies may well be preferentially absorbed compared to the linear scatter from the fundamental (although an increase in attenuation with frequency should not be taken for granted in bubble clouds, as it will tend to peak around the main resonance of the population).

The example shown above (Fig. 10) has demonstrated pulse inversion for detection of a target hidden in a bubble cloud by using the scatter from a single bubble, and comparing it with a target which linearly scatters a similar amount of energy to that bubble. The crucial point which it illustrates is that, when using such nonlinear techniques, it is far easier to enhance the scatter from the bubble compared to that of the linear scatterer (a technique not uncommon for use with biomedical ultrasonic contrast agents) than it is to enhance the contrast of the linear scatterer with respect to the scatter from the bubbles. This is because in such cases of contrast enhancement, it is not simply a matter of increasing the signal from the target, but of reducing the signal from the clutter. When the goal is to detect bubbles, the signal in question is nonlinear, and the ‘clutter’ is very small, since there is usually little in the environment which can generate acoustic nonlinearities to such a degree. To illustrate this, consider the ‘sum of responses’ signal in Figure 10. Note that the energy of the ‘clutter’ from the linear scatterers in Fig. 10(b)(i) is, barring digitisation errors, zero, compared to the finite bubble signal in the Fig. 10(d)(i) (which of course has an energy 6 dB greater than the energy of either of the two pulses shown in Fig. 9). As such, the signal-to-noise ratio for using the ‘sum’ signal to detect bubbles is very large indeed. However, when the goal is to detect a linearly scattering target amidst a bubble cloud, the target signal is linear, and the clutter consists of the linear components emitted by the bubble. In most circumstances the linear components are considerable. To illustrate this, consider the formation of the ‘difference’ signal in Fig. 10 in order to detect a linear scatterer amongst bubbles: the energy of the bubble ‘clutter’ in Fig. 10(d)(ii) is -1 dB compared to the energy of either of the two pulses of Fig. 9. Against the same reference, the signal from the linear scatterer in the Fig. 10(b)(ii) is + 6 dB. Therefore whilst using the ‘sum’ signal gave an almost unfeasibly large ratio for contrast enhancement in the detection of bubbles, the ‘difference’ signal gave only a 7 dB enhancement of the linearly-scattering target immersed in a bubble cloud.

The absolute value of the dB gains is of course arbitrary in this example, which was artificial in two ways. First, the problem was tailored such that the pressures detected from the bubble scatter were similar to those detected from the linear target. Second, only one bubble was present in this simulation, and the insonifying frequency was chosen to be half the bubble's pulsation resonance. Therefore the conditions of this test were set up to promote the generation of a second harmonic of the driving frequency in the bubble pulsations, since this second harmonic would correspond to the bubble pulsation resonance. This optimises the conditions for generating the second harmonic required to make the pulse inversion system work successfully, particularly when the difference signal is used to detect a linear scatterer amongst the bubbles. If a different bubble size were chosen, the enhancement would not be so good, because the energy condition in the even powered harmonics would not be so significant compared to that contained in the linear or odd-powered harmonics. The following section describes a simulation of the operation of TWIPS (Twin Inverted Pulse Sonar) in a real ocean environment, where the target strength is that of a single fish, and the bubble cloud is has a size distribution and void fraction (the proportion of free gas present in a sample of bubbly water) taken from at-sea measurements.

VII. SIMULATION OF TWIPS

To verify the potential for TWIPS to reveal a linearly scattering object within a bubble cloud, a simulation was developed, incorporating three primary elements: a bubble cloud, a target, and an input signal. Details are given in [9]. When present, the target is located at the centre of the cloud and assumed to scatter linearly. This paper uses target strengths of -20 and -25 dB (the latter would be equivalent to Atlantic cod (*Gadus morhua*) broadside to an acoustic beam operating in the frequency regime of interest). The bubble cloud is assumed to be a sphere of radius 1 m, containing around 35 million bubbles following the population size distribution as measured by Meers *et al.* [16], such that the void fractions (the ratio of the volume of gas within a cloud to the total volume occupied by the cloud) on the order of 10^{-7} (i.e. 10^{-5} %).

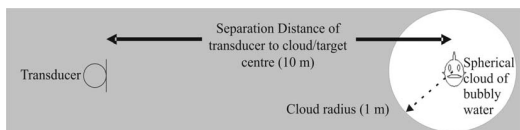


Figure 11. Diagram of simulation geometry for transducer, target and spherical bubble cloud (see [9] for details).

The cloud is dynamic, evolving as a consequence of turbulence, buoyancy *etc.* [1], although the average number and spatial distribution of bubbles is constant. The insonifying wavetrain is shown in Fig. 12(a). It consists of two pulses, identical except that the second (the 'negative' pulse) has opposite polarity to the first (the 'positive' pulse). The amplitudes and frequencies can be found in Leighton *et al.* [9] but are not published for commercial reasons. By splitting the backscattered time series in half and then subtracting the two

half-time-series one from another, scatter from the target can be enhanced with respect to scatter from the bubbles.

The scattered pressure for monostatic operation was calculated from a region of seawater containing spherical cloud of bubbles of radius 1 m, centred on the target (which was at range 10 m from the transducer) (Fig. 11), in order to determine which sonar system could detect whether a target was present in the cloud (See [9] for details). The data presented here are for a single return only, with no averaging. A typical echo is shown in Fig. 12(b): although the time window where the contribution from the target is labelled, it is not possible to see that target.

Fig. 13(a) shows, for the cases where the target is present in the cloud and when it is not, the result of standard sonar processing (cross-correlation of the output pulse with the echo, and averaging over the two echoes corresponding to the scattering of the pair of pulses shown in Fig. 12(a)). The difference is insignificant compared with standard fluctuations in oceanic returns, indicating that standard sonar processing would not be able to identify the presence of the target within the bubble cloud.

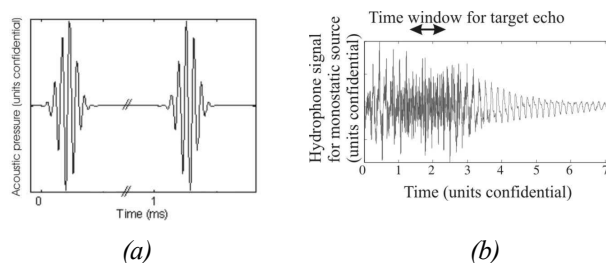


Figure 12. (a) The incident wave (see [9] for details). (b) Simulated monostatic backscatter from the seawater containing a 1 m radius spherical bubble cloud containing, at its centre and 10 m from the transducer, a target (target strength TS = -25 dB). The signals each show a typical return ('positive' pulse only). The signal from the target is buried in bubble noise: the time window in which its echo is received is labelled. See Leighton *et al.* [9] for details.

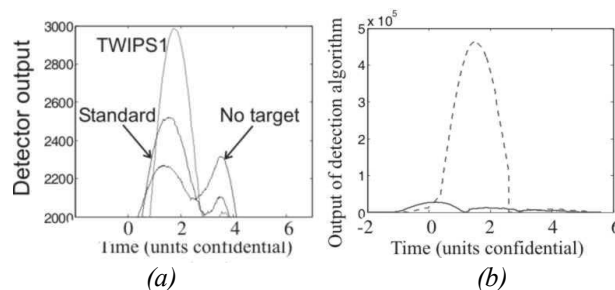


Figure 13. (a) TWIPS1 has been applied to a target of TS=-25 dB using the first of the sonar pulse pairs (the 'positive' pulse) shown in Fig. 12a. The 'standard result' was obtained by normalising the average return of two positive pulses from two different bubble clouds, and cross-correlating that output with the envelope of the input signal. The 'No Target' plot was obtained by performing TWIPS1 on a cloud with no target. In (b), TWIPS2a has been applied to two cases: the bubble cloud on its own (solid line); the bubble cloud with a target of strength TS=-25 at its centre (dashed line). The conditions are identical to those of Fig. 12(b) (which shows the return from the 'positive' pulse only). The target, which was not discernable in Fig. 12(b), gives a signal more than an order of magnitude greater than the scatter from the bubbles. See Leighton *et al.* [9].

Also shown is TWIPS1 processing for the same echoes, which shows a detectable increase over the return from the cloud which does not contain the target. TWIPS1 processing comprises the subtraction of signals shown in Fig. 8.

TWIPS1 gives a reliable but modest increase in target detection, because of the limitations discussed at the end of section VI. However it is possible to do more sophisticated processing of the nonlinearities, all without *a priori* knowledge of either the cloud or the bubble population, to tailor the detection algorithm to the specifics of the transducer platform. Dolphins and porpoises are, for example, able to emit multiple pings in rapid succession. With this ability in mind, other algorithms were generated which sacrifice the reliability of TWIPS1 to gain vastly greater contrast enhancements. An example time series from one example of this generation of TWIPS2 algorithms (specifically, TWIPS2a [9]) is shown in Fig. 13(b): the scatter from the single target fish is more than an order of magnitude greater than from the entire cloud of 35 million bubbles.

In current sonar signal processing, averaging and correlation are used to amplify signals which are consistently found in the same temporal location. Experience has shown that this technique does not yield useful results in the complex, dynamic acoustic environment encountered in a bubble cloud. For the same set of incident pulses, conventional sonar processing was compared with two forms of TWIPS: TWIPS1 and TWIPS2b. TWIPS covers a range of processing techniques, with different capabilities. All are designed to enhance contrast of targets in bubble clouds, both by increasing the scatter from the target and, very importantly, at the same time suppressing the signals from the bubbles. TWIPS1 is designed always to enhance target contrast, producing a reliable enhancement with every ping. TWIPS2b gives much greater contrast enhancements, but not with every ping: the particular form demonstrated here ‘glints’ on about 10% of pings. However the contrast enhancement is much greater than occurs with TWIPS1. It is particularly useful for sources that have the luxury of insonifying a region with multiple pings.

For conventional sonar (Fig. 14(a)), TWIPS1 (Fig. 14(b)) and TWIPS2b (Fig. 14(c)), 50 pulse pairs were projected at the cloud, spaced at intervals of 10 ms. The processed echoes were then stacked, one above each other, to form an image. As a stationary feature in the display, detection of the target in every ping would correspond to the observation of a vertical white line which is visible when the target is present, but absent from the corresponding sonar plot when the target is absent.

The left hand plots in the individual panels of Fig. 14 correspond to the cloud when there is no target present, and the right hand plots of each panel in Fig. 14 correspond to the bubble cloud when the target (TS = -20 dB) is present. In comparing the results, resist the temptation to compare against each other the ‘target present’ plots in (a)-(c). Rather, mimic the consideration of a sonar operator: Recalling that the same echo can be processed by conventional and TWIPS techniques simultaneously, consider the difference between the left and right plots in each panel, and ask whether a sonar operator or dolphin or porpoise could tell, from the left panel, that a target

was absent; and from the right, whether there is a possible target to investigate.

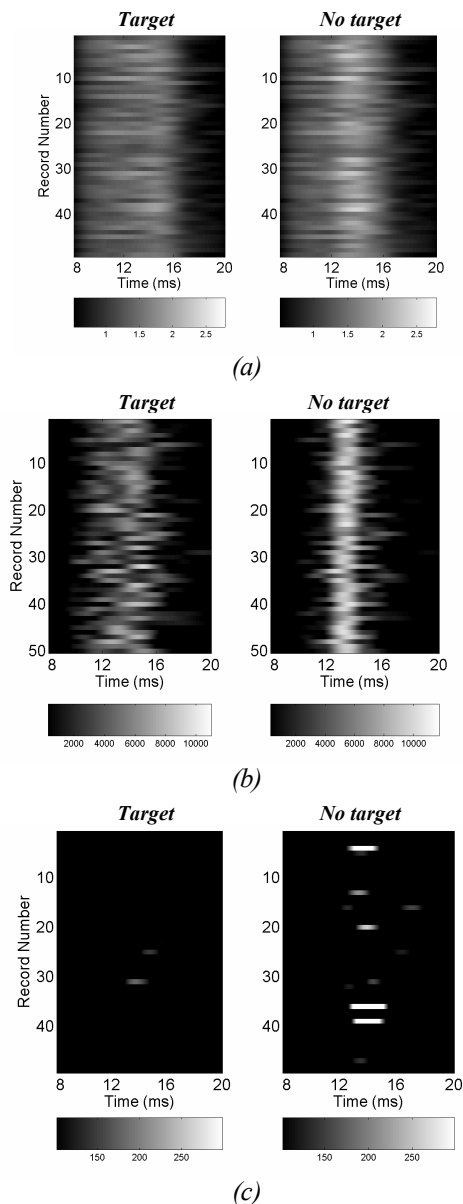


Figure 14. Fifty pulse pairs were projected at the cloud, spaced at intervals of 10 ms, and the echoes processed using (a) conventional sonar deconvolution techniques, (b) TWIPS1 and (c) TWIPS2b. The left plot in each panel shows the case when there is no target present, and the right plot shows the case when a target is inserted at the cloud centre (TS = -20 dB). The cloud, of 1 m radius, contains 35 million bubbles, and evolves appropriately between each ping, as described earlier (Fig. 11). (a) A single average was formed from the two pulses that make up each pulse pair, such that 50 averages are available for plotting. Each average was plotted as a time history on a one-dimensional line, with a greyscale such that the amplitude of the signal at the corresponding moment in the time history was displayed. These processed echo time histories were then stacked, one above each other, to form an image. (b) TWIPS1 processing of the 50 pulse pairs (no averaging) are displayed similarly, by stacking the consecutive grey-scale time series one above the other. (c) TWIPS2b processing is used (no averaging) and the image displayed as in (b). See Leighton *et al.* [9] for details.

Standard sonar processing fails to detect the target: There is insufficient difference between the two plots in Fig. 14(a) because scatter from the bubbles masks the presence of the target. TWIPS1 detects the target on almost every occasion, such that there is a vertical line on the right of Fig. 14(b) compared to the plot on the left (where, importantly, it has suppressed the bubble signal). As stated earlier, TWIPS2 is designed to work spectacularly for about 10% of pings. This feature is shown in Fig. 14(c), in that for some pings it fails to detect the target is present at all. However when it does detect one, the amplitude is very high (see plot on the right); when the target is not present (left hand plot), it rarely delivers a high amplitude return, very effectively suppressing the returned signal. The plots all have a linear greyscale and no thresholding has been applied.



Figure 16. “ (Mar. 18, 2003) -- K-Dog, a Bottle Nose Dolphin belonging to Commander Task Unit (CTU) 55.4.3, leaps out of the water...while training near the *USS Gunston Hall* (LSD 44) in the Arabian Gulf. Attached to the dolphin’s pectoral fin is a ‘pinger’ device that allows the handler to keep track of the dolphin when out of sight. ... units are conducting deep/shallow water mine countermeasure operations to clear shipping lanes for humanitarian relief...” U.S. Navy photo by Photographer’s Mate 1st Class Brien Aho. [Source www.news.navy.mil]

VIII. CONCLUSIONS

The results suggest that the physics will allow nonlinear acoustics to be exploited to enhance the detection of linearly-scattering targets within bubble clouds. Whether or not dolphins and porpoises have developed this faculty, is unknown. It is intriguing that they can generate pulses at amplitudes >50 kPa at ranges of 1 m (even to the point where we might speculate that some of the observed hearing loss over time [17] may be self-induced). Furthermore some species (e.g. *Platanista minor* and *Platanista gangetica*) which can echolocate in highly turbid environments, have lost the ability to use their eyes. As a platform, dolphins and porpoises can approach a target and insonify it with many pulses, the short ranges not only promoting the possible exploitation of nonlinearities, but also allowing relatively small changes in the location of the source to insonify a target from significantly different angles, e.g. through head motion. As regards the specific use of TWIPS, there is some evidence of twin pulses being detected as a result of dolphin and porpoise emissions.

Resolution of this mystery will require careful (preferably open-water) measurements of dolphin and porpoise sonar pulses in turbid and bubbly environments, taking particular

care with measurements of phase. As a result of limitations in state-of-the-art manufactured sonar systems, the spectacular ability for dolphins to detect objects in acoustically complex environments is employed currently by the US Navy for mine-hunting (Fig. 16). The development of technology that matches this extraordinary skill set will offer other options.

REFERENCES

- [1] T. G. Leighton, “From seas to surgeries, from babbling brooks to baby scans: The acoustics of gas bubbles in liquids,” *Int. J. Modern Physics B*, vol. 18, pp. 3267-3314, 2004.
- [2] T. G. Leighton and G. J. Heald, “Chapter 21: Very high frequency coastal acoustics,” in *Acoustical Oceanography: Sound in the Sea*, H. Medwin, Ed. Cambridge University Press, 2005, pp. 518-547.
- [3] T. G. Leighton, P. R. White and D. C. Finfer, “The sounds of seas in space,” *Proc. Int. Conf. Underwater Acoustic Measurements, Technologies and Results*, June 2005, pp. 833-840.
- [4] W. W. L. Au., “The Dolphin Sonar: Excellent capabilities in spite of some mediocre properties” in *High-Frequency Ocean Acoustics*, M. B. Porter., M. Siderius and W. Kuperman, Eds. AIP, NY, 2004 pp. 247-259.
- [5] T. G. Leighton, S. D. Richards and P. R. White, “Trapped within a wall of sound,” *Acoustics Bulletin*, vol. 29, pp. 24-29, 2004.
- [6] H. Williams, *Whale Nation*, Jonathan Cape, London (now Random House), 1988.
- [7] A. Byatt, A. Fothergill, M. Holmes and Sir David Attenborough, *The Blue Planet*, BBC Consumer Publishing (2001).
- [8] K. S. Norris, J. H. Prescott, P. V. Asa-Dorian and P. Perkins, “An experimental demonstration of echolocation behavior in the porpoise, *Tursiops truncatus* (Montagu),” *Biological Bulletin*, vol. 120, 163-176, 1961.
- [9] T. G. Leighton, P. R. White and D. C. Finfer, “Target Detection in Bubbly Water,” *British Patent Application No. 0513031.5* (University of Southampton), 2005.
- [10] K. W. Commander and A. Prosperetti, “Linear pressure waves in bubbly liquids: Comparison between theory and experiments,” *J. Acoust. Soc. Am.*, vol. 85, pp. 732-746, 1989.
- [11] T. G. Leighton, “Surf zone bubble spectrometry: The role of the acoustic cross section,” *J. Acoust. Soc. Am.*, vol. 110(5) Part 2, 2694, 2001.
- [12] T. G. Leighton, S. D. Meers and P. R. White, “Propagation through nonlinear time-dependent bubble clouds, and the estimation of bubble populations from measured acoustic characteristics,” *Proceedings of the Royal Society*, vol. A460(2049), pp. 2521-2550, 2004.
- [13] T. G. Leighton, P. R. White, C. L. Morfey *et al.*, “The effect of reverberation on the damping of bubbles,” *J. Acoust. Soc. Am.*, vol. 112, 1366-1376, 2002.
- [14] T. G. Leighton and H. A. Dumbrell, “New approaches to contrast agent modelling,” *Proc. First Conf. in Advanced Metrology for Ultrasound in Medicine*, *Journal of Physics: Conference Series*, vol. 1, pp. 91-96, 2004.
- [15] T. G. Leighton, P. R. White, D. C. Finfer and S. D. Richards, “Cetacean acoustics in bubbly water,” *Proc. Int. Conf. Underwater Acoustic Measurements, Technologies and Results*, June 2005, pp. 891-898.
- [16] S. D. Meers, T.G. Leighton, J. W. L. Clarke *et al.*, “The importance of bubble ring-up and pulse length in estimating the bubble distribution from propagation measurements,” in *Acoustical Oceanography*, *Proceedings of the Institute of Acoustics*, T. G. Leighton, G. J. Heald, H. Griffiths and G. Griffiths Eds., Bath University Press, 2001, vol. 23(2), pp. 235-241.
- [17] R. L. Brill, P. W. B. Moore, L. A. Dankiewicz, “Assessment of dolphin (*Tursiops truncatus*) auditory sensitivity and hearing loss using jawphones,” *J. Acoust. Soc. Am.*, vol. 109, 1717-1722, 2001.